



# Fault Protection Method of Single-Phase Break for Distribution Network Based on Current Ratio Between Negative and Zero Sequence Current

Xiaohan Li<sup>(✉)</sup>, Tao Tang, Yu Zhou, and Zhongyi Yang

College of Electrical and Information Engineering, Changsha University of Science and Technology, Hunan, China

1357746897@qq.com

**Abstract.** To solve the identification problem of single-phase break fault with power-side grounding (SPBF-PG) and single-phase break fault with load-side grounding (SPBF-LG), a protection method of single-phase break for distribution network is proposed, which is based on current ratio between negative and zero sequence current. The variation characteristics of sequence current of SPBF-PG and SPBF-LG are analyzed by using compound sequence network. Then the protection criterion of negative-zero sequence current amplitude ratio is constructed. This paper presents a new protection method for single-phase break fault (SPBF) which is not affected by line break location, load variation and transition resistance. The method is verified to be correct by simulation.

**Keywords:** Distribution network · Zero sequence current · Negative sequence current · Single-phase break fault

## 1 Introduction

Low-current grounding system is commonly used in medium-voltage distribution network. Interphases short-circuit fault, single line-to-ground fault (SLGF) and SPBF are common faults in low-current grounding system [1]. However, the treatment of SLGF in distribution network has been widely concerned for a long time, but there are few methods to identify and deal with SPBF [2]. Along with the expansion of overhead insulation line laying area and the improvement of lead insulation rate in China's distribution network, overhead insulation line break fault occurs frequently due to lightning strike and other reasons [3]. When the overhead line is struck by lightning, SLGF is caused. The single-phase fault arc continues to burn in the overhead insulated line, and the line at the fault point will be severely oxidized and embrittlement, which will then develop into SPBF, which is easy to affect state of the distribution network and damage the safety of

---

This work was supported by the National Natural Science Foundation of China (52207075).

people and property [4]. Therefore, accurate identification and treatment of SPBF helps to enhance the stability of power grid operation.

SPBF usually include single-phase break and ungrounded fault (SPBUF), SPBF-PG and SPBF-LG. Due to the essential difference between SLGF and SPBF, the existing method of line selection cannot be directly applied to SPBF. The existing methods can detect and isolate faults only one hour after the line falls to the ground, which has some problems, such as delayed information acquisition, low accuracy, and long time for fault resection. Literature [5–7] comprehensively considered the influence of neutral grounding mode, load impedance, transition resistance, line break position and the fault line to earth capacitance and analyzed the neutral voltage migration rules of SPBF. The voltage variation of the three phases before and after the fracture was obtained. Literature [8, 9] puts forward the detection method of SPBF based on artificial intelligence algorithm, which requires large sample data to train the algorithm and depends on the completeness of the information acquisition system. Literature [10] analyzes the law of negative sequence voltage and current and puts forward a method to detect SPBF by using the correlation coefficient of waveform. However, this method is difficult to implement because negative sequence voltages are difficult to measure. Literature [11] deduced the sequence currents of break fault with power side or load side grounding and analyzed the change characteristics and correlation of the sequence current. This method is suitable for small resistance grounding system, but not for small current grounding system because the zero-sequence current does not change obviously.

In this paper, a protection method is proposed which is based on current ratio between negative and zero sequence current. Based on compound sequence network diagram, the expressions of sequence current of SPBF-PG and SPBF-LG are derived. Then the law of the negative and zero sequence current at the head of the fault line and the non-fault line with the transition resistance are analyzed. Thus, the protection criterion of current amplitude ratio between negative and zero sequence current is constructed. Finally, a simulation example is given to verify that the proposed method is not affected by load impedance, line break location and transition resistance value.

## 2 Analysis of SPGF

10 kV distribution network typical structure as shown in Fig. 1.  $\dot{E}_A, \dot{E}_B, \dot{E}_C$  are the three-phase power.  $C_{Aj}, C_{Bj}, C_{Cj}$  are the capacitances to ground of the line  $j$ .  $R_f$  is transition resistance.  $L_P$  is the inductance of arc suppression coil. When the switch K is open, system is the neutral ungrounded system. When it closed, system is a resonant grounding system.

### 2.1 Sequence Current Analysis of SPBF-PG

As shown in Fig. 1, when switch  $K_1$  is closed and  $K_2$  is disconnected, SPBF-PG occurs in the system. Point M on the power side of line  $L_i$  is grounded by the transition resistance  $R_f$ , and a fracture is formed between point M and point N.

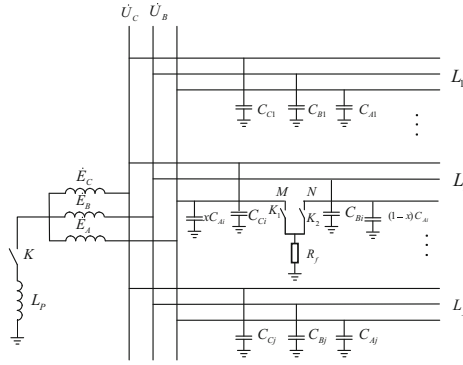


Fig. 1. Equivalent model of 10 kV distribution network.

The voltage at the ground point is transition resistance voltage. The boundary conditions of point M are:

$$\begin{cases} \dot{I}'_{ig1} = \dot{I}'_{ig2} = \dot{I}'_{ig0} \\ \dot{U}'_{iA1} + \dot{U}'_{iA2} + \dot{U}'_{iA0} = 3\dot{I}'_{ig0}R_f \end{cases} \quad (1)$$

where,  $\dot{I}'_{ig1}$ ,  $\dot{I}'_{ig2}$ ,  $\dot{I}'_{ig0}$  are the positive, negative and zero sequence currents of ground point in SPBF-PG.  $\dot{U}'_{iA1}$ ,  $\dot{U}'_{iA2}$ ,  $\dot{U}'_{iA0}$  are the positive, negative and zero sequence voltage of ground point.

The current of fault line at the break point is 0. The boundary conditions of point N are:

$$\begin{cases} \dot{I}'_{i11} + \dot{I}'_{i12} + \dot{I}'_{i10} = 0 \\ \Delta\dot{U}'_{iA1} = \Delta\dot{U}'_{iA2} = \Delta\dot{U}'_{iA0} \end{cases} \quad (2)$$

where,  $\dot{I}'_{i11}$ ,  $\dot{I}'_{i12}$ ,  $\dot{I}'_{i10}$  are the positive, negative and zero sequence currents at the breakpoint of SPBF-PG.  $\Delta\dot{U}'_{iA1}$ ,  $\Delta\dot{U}'_{iA2}$ ,  $\Delta\dot{U}'_{iA0}$  are the positive, negative and zero sequence voltage at the breakpoint.

According to Eqs. (1) and (2), the compound sequence network of SPBF-PG can be obtained, as shown in Fig. 2(a). In urban distribution network, the load impedance is large, so the line impedance can be ignored. Where,  $Z_{S1}$ ,  $Z_{S2}$  are the equivalent impedance of positive and negative sequence of the system.  $Z_{iM1}$ ,  $Z_{iM2}$  are the positive and negative sequence impedances upstream of the breakpoint.  $Z_{iL1}$ ,  $Z_{iL2}$  are the load impedances from fault line end to breakpoint. In urban distribution network,  $Z_{iL1} = Z_{iL2}$ .  $Z_{j1\Sigma}$ ,  $Z_{j2\Sigma}$  are positive and negative sequence equivalent load impedances of non-fault lines.  $C_{0M}$  is the capacitance upstream of the breakpoint.  $C_{iL}$  is the capacitance downstream of the breakpoint.  $C_{j1\Sigma}$  is all of the capacitors of all non-fault lines.

In fault line, the expression of each sequence current can be obtained according to the compound sequence network of SPBF-PG:

$$\begin{cases} \dot{I}'_{i2} = \frac{1/Z_{S2} + 1/Z_{j2\Sigma}}{1/Z_{S2} + 1/Z_{iM2} + 1/Z_{j2\Sigma}} \left( \frac{\dot{E}_A}{3R_g + Z_0} - \frac{\dot{E}_A}{2Z_{iL2}} \right) \\ \dot{I}'_{i0} = \frac{j\omega C_{j\Sigma} + 1/3Z_g}{1/3Z_g + j\omega C_{j\Sigma} + j\omega C_{iM}} \frac{\dot{E}_A}{3R_g + Z_0} \end{cases} \quad (3)$$

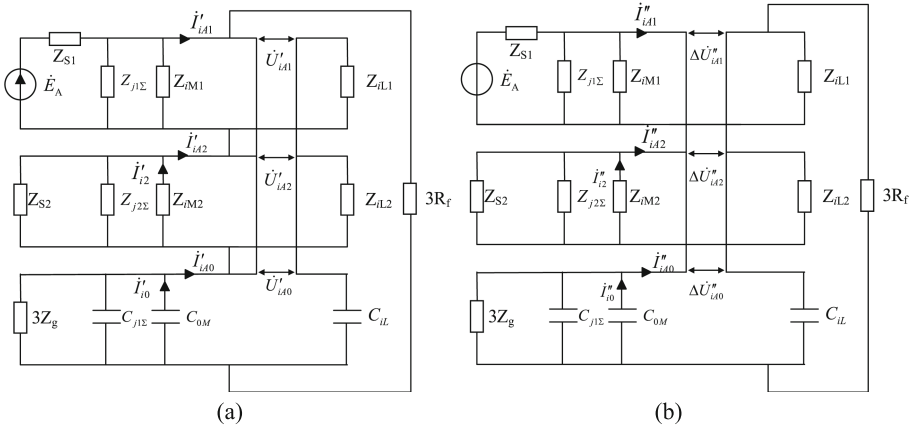


**Fig. 2.** The compound sequence network of SPBF-PG and SPBF-LG. (a) SPBF-PG.(b) SPBF-LG.

Assuming that  $\dot{I}'_2$  and  $\dot{I}'_0$  are two components of negative sequence current, the expressions of  $\dot{I}'_2$  and  $\dot{I}'_0$  are as follows:

$$\begin{cases} \dot{I}'_2 = \frac{\dot{E}_A}{2Z_{iL2}} \\ \dot{I}'_0 = \frac{\dot{E}_A}{3R_f + Z_0} \end{cases} \quad (4)$$

According to the formula, the change of  $\dot{I}'_2$  mainly depends on  $Z_{iL2}$ . Taking the direction of  $\dot{E}_A$  as a reference, the phase angle of  $\dot{I}'_2$  is equal to the load negative sequence impedance angle, that is,  $\alpha < 26^\circ$ . The change of  $\dot{I}'_2$  is shown in Fig. 3. Its amplitude is about half of the load current before the break. The change of  $\dot{I}'_0$  mainly depends on  $R_f$ . In a neutral ungrounded system, the phase angle of  $\dot{I}'_0$  is:

$$\beta = \arctan\left(\frac{1}{3R_f \omega C_0}\right) \quad (5)$$

where,  $C_0 = \sum_{j=1, j \neq i}^n C_j + C_{iM}$ .

In an arc suppression coil grounding system, the phase angle of  $\dot{I}'_0$  is:

$$\beta = \arctan\left(\frac{3\omega^3 C_0 L^2 - \omega L}{R_f(1 + 9\omega^4 C_0^2 L - 6\omega^3 C_0 L)}\right) \quad (6)$$

Combined with Eqs. (5) and (6), with the increase of transition resistance  $R_f$ , the phase angle and amplitude of  $\dot{I}'_0$  decrease. The change in  $\dot{I}'_0$  is shown in Fig. 3.

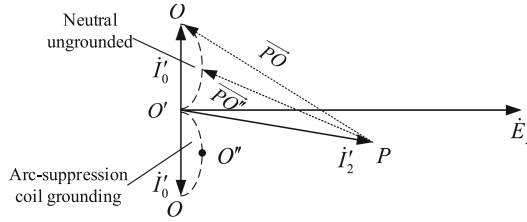


Fig. 3. The change of the negative sequence current in SPBF-PG.

When the transition resistance  $R_f$  is 0, the amplitude of  $\dot{I}'_0$  reaches the maximum value  $|\dot{E}_A / Z_0|$ . The phase Angle  $\beta$  is also at its maximum, and  $\dot{I}'_0$  points to  $O$ . When the transition resistance  $R_f$  approaches infinity, the amplitude and the phase angle approach zero.

Therefore, as the transition resistance increases,  $\dot{I}'_0$  changes from point  $O$  to  $O'$ , and the negative sequence current  $\dot{I}'_{i2}$  changes from  $\overrightarrow{PO}$  to  $\overrightarrow{PO'}$ . The negative sequence current amplitude decreases first and then increases.

$K_m$  is defined as the current amplitude ratio between negative and zero sequence current. When  $\dot{I}'_{i2}$  is  $\overrightarrow{PO}$ , the amplitude reaches the maximum value. In this case,  $K_m$  is:

$$K_m = \frac{|\dot{I}'_{i2}|}{|\dot{I}'_0|} > 1 \quad (7)$$

When  $\dot{I}'_{i2}$  is  $\overrightarrow{PO'}$ , the negative sequence current value decreases. In this case,  $K_m$  is:

$$K_m = \frac{|\dot{I}'_{i2}|}{|\dot{I}'_0|} > 1 \quad (8)$$

When  $\dot{I}'_{i2}$  is  $\overrightarrow{PO''}$ , the amplitude and phase angle of  $\dot{I}'_0$  both tend to zero. In this case,  $K_m$  is:

$$K_m = \frac{|\dot{I}'_{i2}|}{|\dot{I}'_0|} \approx \infty \quad (9)$$

## 2.2 Sequence Current Analysis of SPBF-LG

As shown in Fig. 1, when switch  $K_2$  is closed and  $K_1$  is disconnected, SPBF-LG occurs in the system. Point N on the load side of line  $L_i$  is grounded by the transition resistance  $R_f$ , and a fracture is formed between point M. The boundary conditions of M and N points are opposite to those of SPBF-PG.

The compound sequence network of SPBF-LG can be obtained, as shown in Fig. 2(b). According to the compound sequence network, the negative and zero sequence current can be expressed as follows:

$$\begin{cases} \dot{I}''_{i2} = \frac{1/Z_{S2} + 1/Z_{j2\Sigma}}{1/Z_{S2} + 1/Z_{iM2} + 1/Z_{j2\Sigma}} \left( \frac{\dot{E}_A}{2(3R_f + Z_0) + 9Z_{iL2}} - \frac{\dot{E}_A}{2Z_{iL2}} \right) \\ \dot{I}''_{i0} = - \frac{j\omega C_{j\Sigma} + 1/3Z_g}{1/3Z_g + j\omega C_{j\Sigma} + j\omega C_{iM}} \frac{\dot{E}_A}{2(3R_f + Z_0) + 9Z_{iL2}} \end{cases} \quad (10)$$

Assuming that  $\dot{I}''_2$  and  $\dot{I}''_0$  are two components of negative sequence current, the expressions of  $\dot{I}''_2$  and  $\dot{I}''_0$  are as follows:

$$\begin{cases} \dot{I}''_2 = \frac{\dot{E}_A}{2Z_{iL2}} \\ \dot{I}''_0 = \frac{\dot{E}_A}{2(3R_f + Z_0) + 9Z_{iL2}} \end{cases} \quad (11)$$

Combining the two equations, at the head of the fault line,  $\dot{I}''_{i2}$  is related to the negative sequence impedance and transition resistance. Whatever the ground resistance is, there's always  $\dot{I}''_2 \gg \dot{I}''_0$ . As the transition resistance increases,  $\dot{I}''_0$  decreases. When SPBF-LG occurs, as the transition resistance increases,  $\dot{I}''_{i2}$  increases. While the zero-sequence current  $\dot{I}''_{i0}$  decreases.

If the transition resistance goes to zero, the negative sequence current is the minimum, and  $K_m$  is the minimum. In this case,  $K_m$  is:

$$K_m = \frac{|\dot{I}''_{i2}|}{|\dot{I}''_0|} = \frac{|7\dot{E}_A/18Z_{iL2}|}{|\dot{E}_A/9Z_{iL2}|} = 3.5 \quad (12)$$

When the transition resistance approaches infinity, the negative sequence current value reaches the maximum, and zero-sequence current is largest. In this case,  $K_m$  is:

$$K_m = \frac{|\dot{I}''_{i2}|}{|\dot{I}''_0|} \approx \frac{|\dot{E}_A/2Z_{iL2}|}{0} \approx \infty \quad (13)$$

### 3 Fault Identification Method Based on Current Ratio Between Negative and Zero Sequence

In the break line of SPBF-PG, as the increase of transition resistance, the negative sequence current shows a trend of first small and then large decreases. While the zero-sequence current decreases. In the break line of SPBF-LG, as the transition resistance increases, negative sequence current decreases while zero sequence current changes in reverse the zero-sequence current decreases. In two kinds of fault, compared with the zero-sequence current, negative sequence current value is larger.

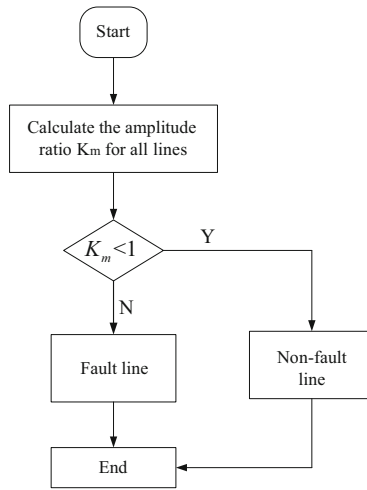


**Fig. 4.** Fault line selection process based on current amplitude ratio between negative and zero sequence current.

Most of the distribution networks are radiation networks, and the load impedance is nearly 100 times the system impedance. That is, most of the negative sequence current flows from break point to source. In the break line, the negative sequence current is at least one magnitude larger than that in the non-break line. The zero-sequence impedance of each component of the system is generally greater than negative sequence impedance numerically. In the non-break line, the zero-sequence current is several times the negative sequence current.

When SPBF-PG or SPBF-LG faults occur,  $K_m$  in the break line is greater than 1. In the non-break line,  $K_m$  is less than 1. The specific line selection process is shown in Fig. 4.

### 4 Simulation and Verification

To verify that the method is correct, the typical structure of 10kV distribution network as shown in Fig. 1 was established based on Matlab/Simulink. It has 6 lines, which adopt

neutral ungrounded system. The line length and load are shown in Table 1. Positive sequence and zero sequence parameters of the line are:  $R_1 = 0.031 \Omega/\text{km}$ ,  $L_1 = 0.096 \text{ mH}/\text{km}$ ,  $C_1 = 0.338 \mu\text{F}/\text{km}$ ,  $R_0 = 0.234 \Omega/\text{km}$ ,  $L_0 = 0.355 \text{ mH}/\text{km}$ ,  $C_0 = 0.265 \mu\text{F}/\text{km}$ .

**Table 1.** Line and load parameters.

Line number	Length (km)	Load size (MW)
1	10	1
2	10	2
3	7	1
4	5	2
5	5	1
6	8	0.5

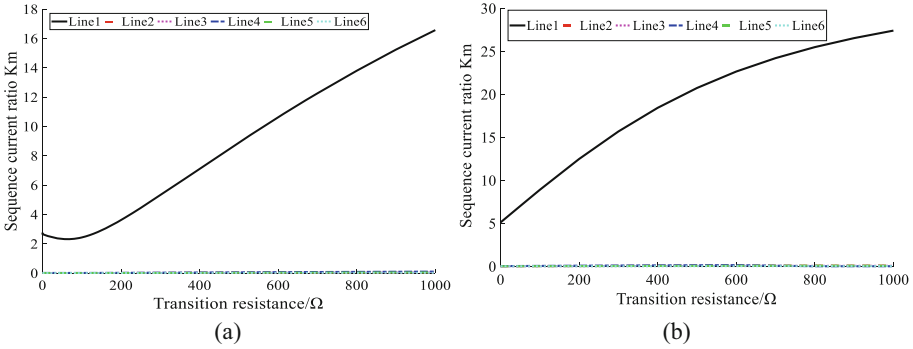


**Fig. 5.**  $K_m$  of each line varies with the transition resistance. (a)SPBF-PG. (b)SPBF-LG.

SPBF-PG and SPBF-LG are respectively set at 5km of line L1.  $K_m$  of each line with the change of transition resistance is shown in Fig. 5. With the change of transition resistance, the  $K_m$  of the break line is always much larger than that of the non- break line in the two faults. In non-fault line,  $K_m$  is always less than 0.1. In SPBF-PG, the  $K_m$  of the fault line decreases first and then increases, and the minimum  $K_m$  value is 2.3. In SPBF-LG,  $K_m$  increases continuously from 5.

In the case of 0, 100, 300 and 500  $\Omega$  transition resistance respectively, change the fault position of line L1. The variation of  $K_m$  of the break line L1 and non-break line L2 can be obtained as shown in Fig. 6. At different fault locations,  $K_m$  of the fault line changes little, and  $K_m$  is always greater than 1. In non-fault line,  $K_m$  is less than 1.

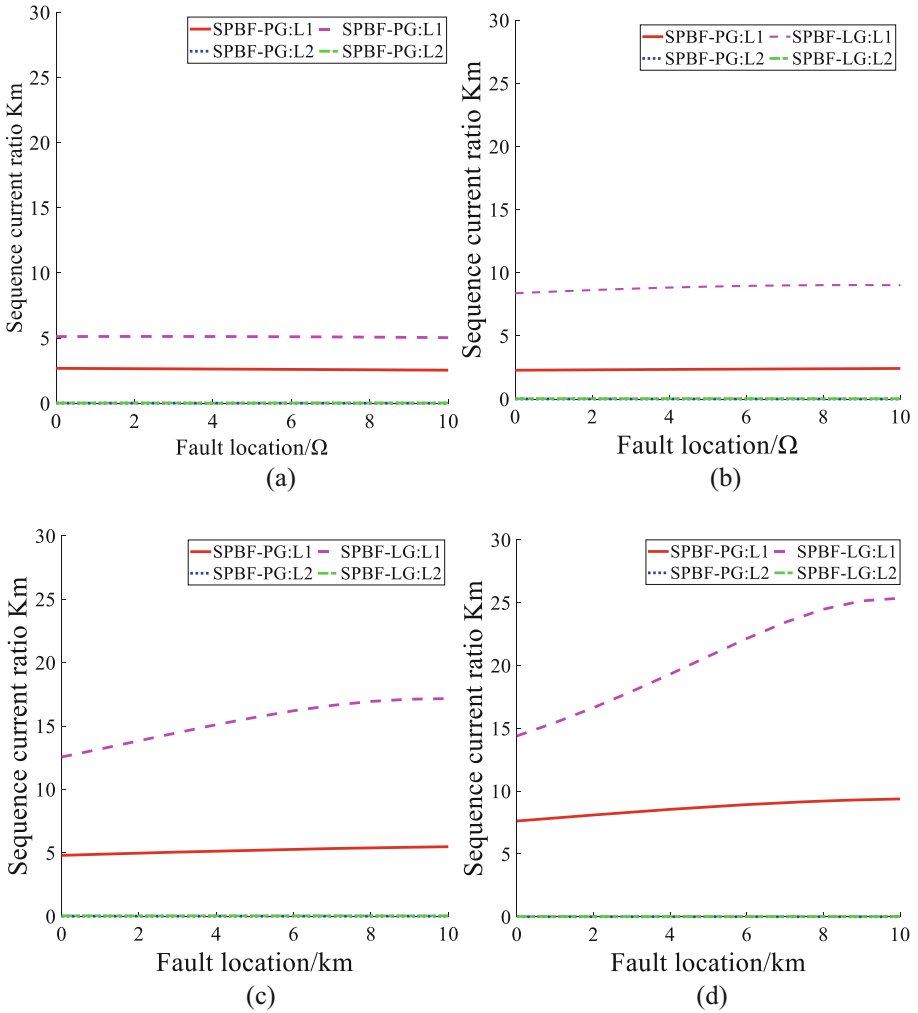


**Fig. 6.** The influence of position change on  $K_m$  under different transition resistance (a) 0Ω. (b) 100Ω. (c)300Ω. (d) 500Ω.

To explore the influence of load distribution on  $K_m$ , two groups of different loads were connected to the system respectively. In the first group, 1 WM load is set at 2 km of line L1; 2 WM Load is set at 5 km of line L2; 2 WM Load is set at 6 km of line L5. In the second group, 1 WM load is set at 7 km of line L1; 0.5WM Load is set at 4 km of line L3; 1 WM Load is set at 1 km of line L4. SPBF-PG and SPBF-LG occurred at 5km of line L1, and  $K_m$  of the fault line L1 and non-fault line L2 changes with transition resistance as shown in Fig. 7. Increasing load behind breakpoint has great influence on the  $K_m$  of the fault line. As the load increases, the negative sequence current of increases, so does the  $K_m$ . No matter how the load changes, the method can still distinguish the fault line accurately.

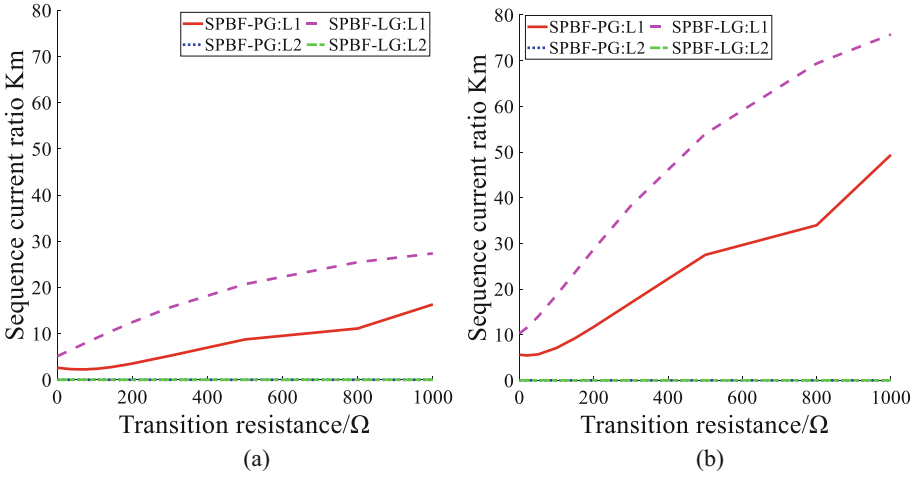


**Fig. 7.** Variation of  $K_m$  under different loads (a) The first group. (b) The second group.

## 5 Conclusion

This paper studies the changes of negative sequence current and zero sequence current after SPBF-PG and SPBF-LG occur. Based on the difference in the distribution of sequence current between faulty and non-faulty lines, this paper put forward a fault protection method based on current ratio between negative and zero sequence current. The method only needs to collect the sequence current of the line, and the faulty line under SPBF-PG and SPBF-LG can be selected by comparing the current ratio of each line. Simulation proves that this method is not affected by break location, load change and transition resistance and has higher sensitivity and reliability.

## References

1. Tang, T., Huang, C., Li, Z., Yuan, X.: Identifying faulty feeder for single-phase high impedance fault in resonant grounding distribution system. *Energies* **12**, 598 (2019)
2. Wang, S., Zhang, H., Xu, B.: Diagnosis of the type of single-phase disconnection and ground fault in the small current grounding system. *Electr. Power Autom. Equipment* **38**(7), 134–139+147 (2018)
3. Wang, M., Lv, Y., Zou, H.: Analysis of lightning-caused break mechanism of 10 kV insulation-covered conductors and its countermeasures. *High Voltage Eng.* **33**(1), 102–105 (2007)
4. Shen, H., Chen, W., Wang, S.: Simulation tests on lightning stroke-caused wire-breakage of 10 kV overhead transmission line. *Power Syst. Technol.* **35**(01), 117–121 (2011)
5. Xue, Y., Chen, M., Cao, L.: Analysis of voltage characteristics of single-phase disconnection fault in ungrounded distribution system. *Proc. CSEE* **41**(4), 1322–1333 (2021)
6. Zhang, L., Cao, L., Li, L.: Analysis and fault section location of single-phase open fault for ungrounding system. *Power Syst. Prot. Control* **46**(16), 1–7 (2018)
7. Zhang, H., Cao, L., Feng, G.: Analysis of single-phase open fault for resonant grounded system. *Proc. CSU-EPSSA* **31**(2), 58–65 (2019)

8. Suwo, W., Zhang, Y., Yun, S.: Open-line fault diagnosis based on data association of MV distribution network. *Electr. Power Autom. Equipment* **37**(7), 101–109 (2017)
9. Guo, N., Yun, S., Tian, Y.: Disconnected unground fault detection in medium voltage distribution network based on FC-AdaBoost. *Electr. Meas. Instrum.* **56**(16), 1–6 (2019)
10. Chang, Z., Song, G., Zhang, W.: Characteristic analysis and fault segment location on negative sequence voltage and current of single-phase line breakage fault in distribution network. *Power Syst. Technol.* **44**(8), 3065–3072 (2020)
11. Xiao, Y., Ouyang, J., Xiong, X.: Protection method of compound break fault with grounding for distribution network considering influence of fault resistance. *Power Syst. Technol.* **45**(11), 4296–4307 (2021)